Formation of H($n = 2$) atoms by the nearly resonant process H^+ in Cs. Multiple collision processes

P. Pradel, F. Roussel, A. S. Schlachter, G. Spiess, and A. Valance
Service de Physique Atomique, Centre d'Etudes Nucléaires de Saclay, 91190 Gif-sur-Yvette, France
(Received 16 April 1974)

Formation of H atoms in the $n = 2$ states for the nearly resonant charge-transfer process $H^+ + Cs$ (energy defect: 0.49 eV) is studied in the energy range 0.25–3.0 keV. The outgoing H($2S$) atoms are quenched in a transverse electric field. The cross section for formation of H($2S$) atoms exhibits typical nearly resonant characteristics. The principal maximum, $(6.0 \pm 0.25) \times 10^{-15}$ cm^2 occurs at 0.5-keV H^+ energy; a secondary maximum is observed at 1.35 keV. Structure is discussed in terms of the potential-energy curves of the quasimolecule $(CsH)^+$. The cross section for formation of H($2P$) atoms is obtained by an indirect method. The H($2S$) fraction f relative to the outgoing neutral beam for a thin Cs target is obtained; f is close to the statistical value of 0.25 for H^+ energies greater than 1 keV, and has a maximum value of 0.55 ± 0.075 at 0.6 keV. Multiple collisions are studied for Cs targets of variable thickness. The H($2S$) fractional yield F_m relative to the total outgoing beam has a maximum for a Cs target thickness of about 10^{14} atoms/cm^2. The largest value of F_m is 0.30 at 0.5 keV. F_m approaches zero as an equilibrium value. A four-component charge-exchange model is used to show that the primary destruction mechanism of H($2S$) atoms is collisional deexcitation, with a cross section of about 5×10^{-15} cm^2. The influence of scattering and calibration of a secondary-emission neutral detector are discussed. Finally, the polarization P of Lyman-α radiation from quenching of H($2S$) atoms in a transverse electric field is measured as a function of applied electric field. P is negative, varying from -0.31 ± 0.03 in a near-zero electric field to -0.50 ± 0.06 for a field of 475 V/cm. Data are in agreement with an adiabatic theory; in addition, oscillations about the theoretical curve are observed.

I. INTRODUCTION

Formation of a beam of hydrogen atoms in the metastable 2S state by the nearly resonant charge-exchange process

$$H^+ + Cs \rightarrow H(2S) + Cs^+ \quad (\Delta E = -0.49 \text{ eV}) \qquad (1)$$

was first studied by Donnally *et al.*[1] and later by others.[2,3] The small energy defect results in a large cross section for this collision at a low proton energy, and provides a means of obtaining an intense metastable hydrogen beam.

An important application of Eq. (1) in nuclear physics is in polarized ion sources of the Lamb-shift type,[2,4-7] which results in polarized H^+ or H^- beams having a larger intensity than in ground-state ion sources (those using separation of hyperfine states of ground-state H in an inhomogeneous magnetic field). In a Lamb-shift–type polarized ion source, polarization is obtained by selective quenching of certain hyperfine substates of H(2S) in suitable electric and magnetic fields. Metastable atoms then undergo selective electron attachment or detachment in a collision in an appropriate target gas.

Secondly, there is recent increasing interest in charge-exchange processes involving alkali-metal atoms.[8-11] The theory of such processes, including resonant[12] and nonresonant charge transfer[13-15] has been developed in the impact parameter formulation.[16] In these systems, consisting of many-electron atoms, the main part of the charge-exchange cross section is due to the valence electron. The interaction between the active electron and the remaining core electrons may be replaced by an appropriate pseudopotential[17,18] so that the collision is treated as a one-electron problem.

The following subscript notation is used in this paper: +, −, m, r, g, and 0 refer, respectively, to H^+, H^-, and H^0 in the metastable 2S state, H^0 in the radiative 2P states, H^0 in the ground state (or, when used as a second subscript, in the ground state or in a state which decays to the ground state by an electric dipole transition), and H^0 in any state. [A more usual notation for r is 2P, but this is not consistent with the use of m for 2S; furthermore, as reaction (1) is also nearly resonant for formation of the 2P states, the use of r rather than g emphasizes the role of the 2P states.] Thus, for example, σ_{mg} is the cross section for collisional deexcitation of an atom in the H(2S) state. The metastable fraction f is the fraction of H(2S) atoms in the neutral beam as the result of a collision of a proton in a thin Cs target (more precisely defined in Sec. IV B 6).

It is well known that the field-free lifetime of an H atom in the metastable 2S state is $\tau_m = 0.14$ sec (two-photon emission), since decay by electric dipole and quadrupole transitions to the ground state is forbidden and since the decay rate by mag-

netic radiation is very small. The $2P$ states decay by electric dipole radiation to the ground state. The lifetime is very short: $\tau_r = 1.6\times10^{-9}$ sec. The photon from the decay from $n=2$ to the ground state is called Lyman α, and has a wavelength of 1216 Å. The $2S_{1/2}$ state lies above the $2P_{1/2}$ state in energy; the separation is, however, very small (the Lamb shift, which corresponds to an energy of 4.4×10^{-6} eV). Spontaneous decay from the $2S_{1/2}$ state to the $2P_{1/2}$ state could occur; the probability is, however, negligible because of the small energy difference. In the presence of an external electric field, Stark mixing of the $2S$ state with the $2P$ states occurs, leading to rapid decay of the $2S$ state with the resulting emission of a Lyman-α photon; this process is called quenching. The lifetime of the $2S$ state as a function of applied electric field has been calculated.[19] In a very strong electric field, the lifetime of the $2S$ state approaches twice that of the $2P$ states. A field of 500 V/cm is sufficient to reduce the $2S$ lifetime to 5.6×10^{-9} sec. The lifetime of the $2P$ states increases slightly in an electric field. Lifetimes of the $2S$ and $2P$ states are also affected by a magnetic field.

This paper presents an absolute measurement of the cross section σ_{+m} in the energy range 0.25–3.0 keV. Although this cross section has been previously measured,[1-3] the results can be criticized because of dubious calibration or normalization procedures. Indeed, previous results give values which differ by as much as two orders of magnitude at a given energy. The authors have previously published a measurement of σ_{+m},[20] but for only one energy, 2.4 keV. Thus, in this paper, the energy range is considerably extended, and includes the energy range in which σ_{+m} has its maximum value. In addition, we present estimated values for the cross section σ_{+r}. A model is proposed to explain structure observed in the cross section σ_{+m}.

The cross section σ_{+0} has been previously measured[20-25] in a very wide energy range. Reported values are generally in good agreement at low energy (up to 5 keV); values at higher energies show rather poor agreement.

The metastable fraction f has recently been reported in a companion experiment by Tuan *et al.*[26,27] In the experiment of Tuan *et al.*, f was directly determined by measuring Lyman-α radiation in the collision zone with and without an applied quenching field. In the present experiment the metastable atoms leave the collision zone and are subsequently quenched. Values of f for the two experiments are compared.

The influence of multiple collisions, particularly on the destruction of atoms in the $2S$ state, is studied by using a thick Cs target and a charge-exchange model. Results are reported for σ_{mg}.

The Lyman-α radiation from the quenching of H(2S) atoms in an external electric field is known to be polarized.[28-35] We present results for this polarization as a function of applied electric field for fields up to 500 V/cm. Comparison is made with a previous measurement and with an adiabatic theory.[33] Structure is observed, and an explanation is proposed. This polarization is not only of basic interest but can be used to correct other measurements made using quenching of H(2S) in an electric field; the correction is non-negligible for field strengths and observation angles commonly employed.

Calibration of a secondary-emission neutral-atom detector for incident ground-state H atoms is presented for energies between 0.5 and 3.0 keV. This has been previously reported only at much higher energies.[36-40] This calibration was necessary for the present experiment, but could be useful for other experiments as well, as the results seem to be general.

Portions of the present results have been previously reported.[20]

II. APPARATUS

A. General description

A schematic diagram of the apparatus is shown in Fig. 1. A proton beam is extracted from a duoplasmatron source and is focused by an einzel lens. It is magnetically mass analyzed and suitably collimated before entering a cell containing Cs vapor where charge-exchange processes occur. After the cell the beam passes through a drift region where the ions can be removed from the beam with a weak transverse electric field without appreciable quenching of the metastable atoms. A strong electric field can also be applied in the drift region, which then serves as a prequenching system in order to test the efficiency of the quenching assembly. The quenching assembly is composed of an electrostatic quadrupole. The Lyman-α photons, emitted by the Stark-quenched H(2S) atoms, are detected by a channel electron multiplier. The beam then passes through a magnetic field to separate the H^+, H^0, and H^- components, which are detected using two Faraday cups and a secondary-emission neutral-atom detector. Typical background pressure in the vacuum system is of the order of 10^{-7} Torr.

B. Proton beam

The proton beam is extracted from a duoplasmatron source through a 0.2-mm hole, accelerated

by an electrode negatively biased, and decelerated by a ground potential electrode which is also the first electrode of the einzel lens. The measured H^+-beam energy spread is about 5 eV. The H^+ beam is mass analyzed by a 90° deviation in a magnetic field. It is then collimated by two diaphragms, 1.5 mm in diameter and 76 cm apart. Spurious effects due to the fringing field of the magnetic analyzer are minimized by careful shielding. Earth's magnetic field is compensated for by passing a suitable current in a long rectangular coil surrounding the entire apparatus. The residual magnetic field is measured to be smaller than 0.01 G between the diaphragms and smaller than 0.02 G downstream from the second diaphragm. The deviation of the H^+ beam from a straight line due to stray magnetic field does not exceed 0.3 mm per meter of path at 0.5 keV. Care was taken to ensure that no insulating surfaces were in direct view of the beam.

The geometrical beam divergence (half-angle) is 0.11° and the measured beam full width at half-maximum is only 0.08°. All the other diaphragms have acceptances greater than the geometrical beam divergence. The acceptance of the detectors, located at the end of the apparatus, is 0.33°, as seen from the Cs cell. In Secs. IV B 1 and V A the influence of scattering in the Cs cell is discussed.

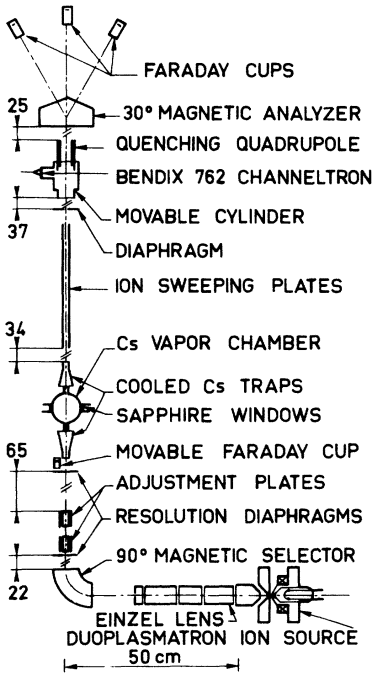

FIG. 1. Schematic diagram of the apparatus. The chambers are drawn to scale. The spaces between them are indicated in cm in the figure. The resolution diaphragms are 1.5 mm in diameter, 76 cm apart.

C. Cesium cell

The Cs cell has been extensively described in a previous paper.[20] As shown in Fig. 2, the cell is loaded with 2 g of Cs under vacuum and is homogeneously heated either at a given controlled temperature or at a constant rate of increase of temperature. During a series of measurements the Cs vapor density is measured by the absorption of resonant $(6P_{3/2}\text{-}6S_{1/2})$Cs light emitted by a spectral lamp. A calibration procedure described in Ref. 20 and absolute measurements[41] show that the Cs density does not vary more than 5%.

The rate of Cs loss from the cell is minimized by two heated copper tubes, 4 mm (entry) and 4.5 mm (exit) in diameter and 37 mm long, located on the beam axis. At a temperature of about 100°C, 2 g of Cs last several months. Two freon-cooled traps located on the beam axis protect the remainder of the apparatus from Cs contamination.

D. Quenching assembly

Metastable hydrogen atoms are detected by applying a strong transverse electric field which induces Stark mixing between the $2S_{1/2}$, $2P_{1/2}$, and $2P_{3/2}$ states of hydrogen, resulting in the emission of a Lyman-α photon. The electric quench field

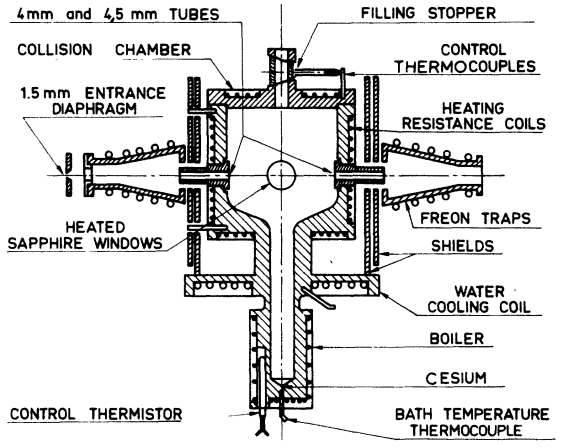

FIG. 2. Scaled drawing of the cesium cell. The cell is made of pure copper. Temperatures of the boiler and of the chamber are controlled and adjustable. The Cs vapor density is measured by the absorption of resonant light emitted by a Cs spectral lamp.

is the fringing field in front of two parallel plates 65 mm long and 40 mm wide biased at opposite potentials with respect to ground. The gradient of this fringing field is increased by two image plates located 3 mm outside the inner plates. This ensures that the quenching of the H(2S) atoms occurs in a small region of beam in the field of view of the detector. A plot of the field lines, obtained by numerical integration of Laplace's equation in two dimensions, shows that the gradient of the fringing field is very large when the outer plates are 4 mm longer than the inner plates. In this case a zero-field point appears on the axis of the beam 25 mm in front of the edge of the outer plates.[20] A discussion of the detection efficiency is given in Ref. 20. The photon detector is a precalibrated Bendix 762 Channeltron operating in a counting mode. Knowing the solid angle ($\Omega = 2.33 \times 10^{-2}$ sr) of the detector photocathode viewed from the emitting beam region, the H(2S) atom intensity in the beam is known to be

$$I_m = 4\pi Ne/\Omega\eta, \tag{2}$$

where N is the counting rate at the anode of the detector and η is the quantum efficiency of the detector at the Lyman-α wavelength ($\eta = 0.107$, furnished by the manufacturer).

Formula (2) neglects the correction for the polarization of the Lyman-α radiation, i.e., the spatial anisotropy of the photon intensity with respect to the direction of the quench electric field. It is well known[28,29] that the magnitude of the correction depends on the geometry of the quenching system and the time required for the H(2S) atoms to enter the quench field. Up to now, some absolute measurements of H(2S) atom intensity described in the literature[42-44] have not taken into account the polarization correction because an investigation, adapted to each field configuration, is necessary to apply such a correction. As the correction may be large, we have carefully studied the polarization of the Lyman-α radiation in our quenching system. The subject is treated in Sec. III B.

E. Particle detectors

The initial proton beam intensity I_+^0 is measured with a retractable Faraday cup located just behind the second collimating diaphragm. After the quenching region a 30° magnetic analyzer deviates the residual protons and the negative hydrogen ions, which are detected by two Faraday cups 25 mm in diameter. The Faraday-cup guard rings are biased at −45 V with respect to ground. It was verified that an increase of the bias potential does not appreciably change the measured current.

The neutral-particle detector, located on the axis of the beam, is a stainless steel cup with a concentric ring in front biased at +45 V to attract the secondary electrons. This detector has to be calibrated for both ground-state and metastable hydrogen atoms. In Sec. III A the secondary-emission coefficients are investigated for "dirty" stainless steel in the energy range of interest.

III. CALIBRATIONS

A. Calibration of the neutral atom detector

While it is easy to measure the secondary-emission coefficient γ_+ for protons by inverting the guard-ring bias potential of a Faraday cup, care must be taken to obtain the secondary-emission coefficient γ_g for ground-state hydrogen atoms, which is not necessarily the same as γ_+. The usual results cited[36-40] give the ratio γ_g/γ_+ for hydrogen on nickel, beryllium, copper, and silver magnesium surfaces for energies greater than 8 keV. The average value of $\gamma_g/\gamma_+ = 1.11 + 0.001E$, where the energy E is in keV. These values are often extrapolated to lower energies and used for other surfaces.[44] It was pointed out by Barnett and Ray[40] that the ratio of the emission coefficients γ_g/γ_+ is apparently independent of the target surface and the angle of incidence. However, it is not expected to remain close to 1.11 at lower energies because the secondary-emission mechanism depends on the energy.[45]

In order to correctly calibrate the neutral detector, γ_+ and γ_g have been independently measured in the energy range 0.5–3 keV. A cell containing argon was mounted on the beam axis between the quenching region and the detectors. When the argon target thickness Π_{Ar} is low enough to ensure single collisions, the charge-exchange reaction of the incident H^+ in Ar produces a linear decrease of the H^+ intensity I_+ and a corresponding linear increase of the H(1S) atom intensity I_g. The ratio of the two linear variations $\Delta I_g/\Delta I_+$, when Π_{Ar} is varied, is equal to the secondary-emission coefficient γ_g for neutral hydrogen atoms in the ground state. The formation of metastable hydrogen atoms in this charge-exchange process is negligible in our energy range because the energy defect of the reaction is much smaller for the H(1S) state (2.2 eV) than for the H(2S) state (12.3 eV). Furthermore, it was verified that negative hydrogen ion formation by a single collision of H^+ in Ar was negligible. An important correction to the intensities must be made to account for scattering of particles at angles larger than θ, the acceptance angle (half-angle) of the detectors. Relative to the argon cell, the acceptance angle was $\theta = 0.5°$. The

measured H^+ intensity, taking into account the proton scattering, is

$$I_+ = I_+^0 \left[1 - \Pi_{Ar}\left(\sigma_{+g} + \int_\theta^\pi \frac{d\sigma_+}{d\Omega}\right)\right], \tag{3}$$

where I_+^0 is the initial H^+ intensity, σ_{+g} is the total inelastic cross section for charge exchange, and $d\sigma_+/d\Omega$ is the elastic differential cross section per unit solid angle Ω for protons. The integral in the second term of Eq. (3) can be calculated for angles larger than the detector acceptance angle. Noting the obvious fact

$$\sigma_{+g} = \int_0^\pi \frac{d\sigma_{+g}}{d\Omega}\, d\Omega, \tag{4}$$

the residual H^+ intensity becomes

$$I_+ = I_+^0 \left\{1 - \Pi_{Ar}\left[\int_0^\theta \frac{d\sigma_{+g}}{d\Omega}\, d\Omega + \int_\theta^\pi \left(\frac{d\sigma_{+g}}{d\Omega} + \frac{d\sigma_+}{d\Omega}\right) d\Omega\right]\right\}, \tag{5}$$

where $(d\sigma_{+g} + d\sigma_+)/d\Omega$ is the total differential cross section $d\sigma_T/d\Omega$ including both elastic and inelastic processes for H^+ in Ar. $d\sigma_T/d\Omega$ has been recently measured by Crandall *et al.*[46] so that it is possible to evaluate the second integral in relation (5).

In the same way, the detector neutral intensity is

$$I_g = \gamma_g I_+^0 \Pi_{Ar} \int_0^\theta \frac{d\sigma_{+g}}{d\Omega}\, d\Omega. \tag{6}$$

Equations (5) and (6) can be combined to eliminate $\int_0^\theta (d\sigma_{+g}/d\Omega)\, d\Omega$. The secondary emission coefficient γ_g is then obtained:

$$\gamma_g = I_g \Big/ \left[I_+^0 - I_+ - \Pi_{Ar} I_+^0 \int_\theta^\pi \frac{d\sigma_T}{d\Omega}\, d\Omega\right]. \tag{7}$$

The third term in the denominator of (7) is the scattering correction where Π_{Ar} and $d\sigma_T/d\Omega$ appear. The target thickness Π_{Ar} is measured with a Baratron differential capacitance manometer. Figure 3(a) shows corrected values of γ_g in the energy range 0.5–3 keV as well as values of γ_+ obtained by simply inverting the guard-ring bias potential of the proton Faraday cup. The bars include all sources of error.

The coefficient γ_+ measured by Bayfield[44] for 2-keV H^+ on "dirty" stainless steel is 2.2, which is in satisfactory agreement with the present value of 1.86. From our results it is seen that γ_g is significantly greater than γ_+ at energies above 0.7 keV. The ratio γ_g/γ_+ [Fig. 3(b)] shows excellent agreement above 1.6 keV with an extrapolation to low energy of Chambers's results.[36] At energies lower than 0.7 keV γ_g is significantly smaller than γ_+ and is expected to be zero for a threshold energy close to 0.35 keV. However, the extrapolated value of γ_+ at zero energy is still 0.3. This behavior is in agreement with theory, which predicts that at low energy, the principal secondary-emission mechanism is the Auger-effect ion neutralization process called potential emission. This process does not occur for incident H(1S) atoms.[45] In conclusion, the ratio γ_g/γ_+ varies and must be measured in order to obtain a reliable calibration of a neutral-hydrogen-atom detector.

To study the secondary-emission coefficient γ_m, metastable hydrogen atoms are created by charge exchange of H^+ in Cs vapor. The secondary electron current from the neutral detector is measured with an incident beam composed of a mixture of H atoms in the 1S state and the 2S state, and with a pure-1S-state atom beam [the H(2S) are quenched before reaching the detector]. No significant variation of the secondary electron current is observed for $E > 0.5$ keV when the H(2S) atoms are quenched. Thus, for dirty stainless steel and for $E > 0.5$ keV the secondary-emission coefficients γ_m and γ_g are taken to be equal. At 0.5 keV, a slight current variation has been ob-

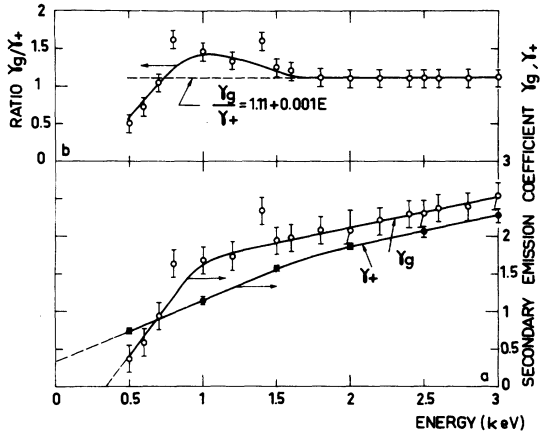

FIG. 3. (a) Secondary emission coefficients for H^+ and H(1S) on "dirty" stainless steel surface at normal incidence. γ_+ is the secondary emission coefficient for incident H^+, γ_g for incident H(1S). A smooth curve has been drawn between the experimental points for clarity. Above 0.7 keV γ_g is significantly greater than γ_+. γ_g is expected to be zero below a threshold energy of about 0.35 keV. The value of γ_+ extrapolated to zero energy is 0.3, which is consistent with an Auger-effect ion-neutralization process. (b) Ratio γ_g/γ_+ from measurements shown in Fig. 3(a). Circles, present work (the error bars include all sources of error); dashed lines, extrapolation to low energy of results of Chambers (Ref. 36) (E is energy in keV). The agreement between the extrapolation of the results of Chambers and the present results is quite good above 1.6 keV.

served; however, the ratio γ_m/γ_g does not exceed 1.04. For deuterium in the ground state, the secondary-emission coefficient is found to be 0.9 at 1 keV.

B. Correction due to polarization of Lyman-α radiation

Quenching of metastable hydrogen atoms in an external electric field is an electric dipole transition. The angular distribution of Lyman-α radiation can be written[30,31]

$$I^{\Theta} = (3I_s/4\pi)[1 - P\cos^2\Theta)/(3 - P)], \qquad (8)$$

where Θ is the angular position relative to the electric quench field direction, P is the polarization of the radiation, and $I_s/4\pi$ is the photon intensity per steradian which would be emitted if the polarization were zero. Once P and Θ are known, from formula (8) one can calculate the photon intensity $I_s/4\pi$ which is needed to obtain σ_{+m}. It is well known that for the so-called "magic angle" Θ_c such that $\cos^2\Theta_c = \frac{1}{3}$ ($\Theta_c = 54°44'$), the emitted radiation is independent of P. In all our measurements the photon detector was placed at the "magic angle" so that polarization does not affect the cross section for production of H(2S) atoms.

As polarization necessitates a correction when a photon detector is located at an angular position other than Θ_c, it is interesting to measure P for quenching in a transverse electric field with finite gradient. Such an investigation may be useful in order to correct other measurements when polarization has been neglected (photon measurement at 0° or 90° are often made).

Polarization in a weak electric field has been measured experimentally by Fite *et al.*[30] and by Spiess *et al.*[20]; measured values are, respectively, -0.30 ± 0.02 and -0.31 ± 0.03. The theoretical value taking account of the hyperfine structure of hydrogen[32] is -0.3233 ± 0.0004. The agreement is very good. For intermediate electric fields the polarization depends on the strength of the field and on the way the H(2S) atoms enter the field. The polarization has been calculated for two extreme cases: adiabatic entry of the H(2S) atoms into the field[33] and sudden entry.[34] Entry is called adiabatic under the following conditions. For an H(2S) atom beam, the time-dependent energy perturbation $V(t)$ is due to an electric field, and the states which are primarily mixed with the $2S_{1/2}$ state are the $2P_{3/2}$ and the $2P_{1/2}$ states. The elements of the Hamiltonian which mix the unperturbed states are given by[35]

$$V_1(t) = \langle 2P_{3/2}|e\vec{\mathbf{E}}\cdot\vec{\mathbf{r}}|2S_{1/2}\rangle = -\sqrt{6}\,E(t)\,ea_0,$$

$$V_2(t) = \langle 2P_{1/2}|e\vec{\mathbf{E}}\cdot\vec{\mathbf{r}}|2S_{1/2}\rangle = \sqrt{3}\,E(t)\,ea_0,$$

where e is the electronic charge, a_0 is the Bohr radius, $e\vec{\mathbf{E}}\cdot\vec{\mathbf{r}}$ is the potential energy of the H(2S) atom in the perturbing electric field $\vec{\mathbf{E}}$, and $\vec{\mathbf{r}}$ is the radius in spherical coordinates. For an H(2S) atom the two natural periods corresponding to the Lamb-shift splitting ($2S_{1/2}$-$2P_{1/2}$) and the fine-structure splitting ($2S_{1/2}$-$2P_{3/2}$) are, respectively, $T_1 = 10^{-9}$ sec and $T_2 = 10^{-10}$ sec. Following Wooten and Macek[35] the entry condition of adiabaticity is always fulfilled if $V_1(t')$ is smaller than the Lamb-shift splitting and if the transit time t' of the H(2S) atom is greater than $T_1(t' = l/v$, where l is the length of the perturbed region and v is the velocity of the H(2S) atom). Our experimental conditions correspond to the adiabatic case. Crandall *et al.*[46] have studied the sudden entry conditions, which are applicable when the H(2S) atoms are formed in the electric field. The only measured values of P for the adiabatic case are those of Sellin *et al.*[33] We have measured polarization for electric fields between 30 and 500 V/cm, a range of values which includes those generally used to quench H(2S) atoms.

From formula (8), P can be determined by detecting the emitted photons successively in directions perpendicular and parallel to an electric quench field whose strength E is known:

$$P(E) = (I^{90} - I^{0})/I^{90}. \qquad (9)$$

For these measurements, the photon detector is mounted on an axial cylinder shown in cross section in Fig. 4. The detector assembly is at ground potential and can be both translated parallel to the beam and rotated through 180° about the beam axis without appreciably perturbing the electric quench field. The quenching assembly described in Sec. II D was slightly modified as follows for the polarization measurements. A 2-mm-diameter aperture[47] located on the beam axis at the entrance to the quenching region ensures that the H(2S) atom beam is well centered on the axis of rotation of the cylinder. In order to have a smaller field gradient, a dipole configuration is used instead of the quadrupole: the two plates on each side of the beam axis are at the same potential, ±3000 V. The dipole configuration simplifies the measurement of the electric field strength because the fringing field rises more slowly with distance from the plates, and does not change the adiabatic nature of the entry of the H(2S) atoms in the field. In front of the photon detector are two slits (2×10 mm and 1×10 mm) (see Fig. 4). The narrower slit is attached to the cylinder at ground potential so that the electric field produced by the fixed plates is not perturbed by the motion of the assembly. All surfaces seen by the detector are cadmium coated to minimize photon reflection.[20] In this

assembly, the photocathode of the detector "sees" a region of the beam only 4 mm long, in which the average value of the electric field can be determined.

Two different methods are used to determine the electric field strength: numerical integration of Laplace's equation in plane coordinates and an indirect experimental method described below.

The photon signal $I^{\Theta}(Z)$ is measured, for a given detector angle Θ, as a function of Z, the position of the detector along the beam axis. The signal $I^{\Theta}(Z)$ is shown in Fig. 5(a) for both the $\Theta = 0°$ and $\Theta = 90°$ angular positions of the detector (Z increasing downstream). As $I^{0}(Z)$ is greater than $I^{90}(Z)$, (9) shows that P remains negative with increasing electric field E. The signal $I^{\Theta}(Z)$ shows a maximum which is easily explained: for small Z the quench field is small and few metastable atoms are quenched, while for large Z almost all the metastable atoms have already been quenched and thus few remain in the beam. At a position Z, where the remaining metastable atom intensity in the beam is $I_m(Z)$, dI_m photons are emitted from the quenching of dI_m metastable atoms in a zone of length dZ. The number of photons counted by the detector is λdI_m, where λ is a coefficient which takes into account the acceptance of the slits, the quantum efficiency of the detector, and the effect of polarization for that angle. For a beam velocity v, the number of quenched atoms in dZ depends on $I_m(Z)$ and the lifetime $\tau_m(E)$ of H(2S) in the field $E(Z)$ existing at Z:

$$dI_m = [I_m(Z)/\tau_m(E)v]dZ. \tag{10}$$

As the electric field and the path length are sufficient to quench essentially all the H(2S) atoms, we can write

$$I_m(Z) = \frac{1}{\lambda}\int_Z^{\infty} I^{\Theta}(Z')dZ'. \tag{11}$$

Relations (10) and (11) give an experimental value for τ_m:

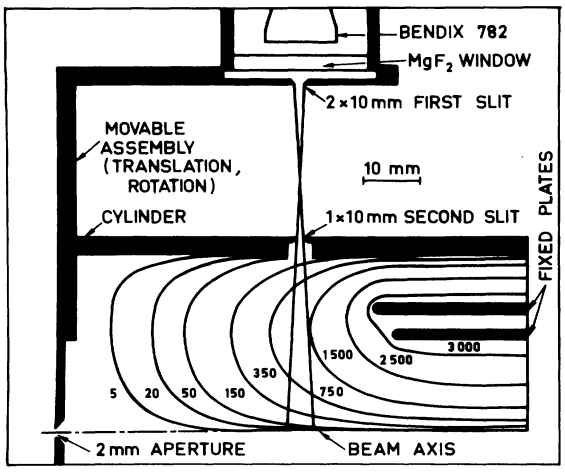

FIG. 4. Configuration of H(2S) detector for measurement of polarization of Ly-α radiation as a function of applied electric field ("dipole configuration"). Equipotential lines shown for 3000 V applied to plates were calculated by numerical integration of Laplace's equation (the plates symmetrically located below the beam axis and biased at −3000 V are not shown). This configuration provides resolution in electric field. A different configuration is used for cross-section measurements: a quadrupole electric quenching field is applied and the slits are removed, the result of which is that essentially all metastable atoms are quenched within the field of view of the photomultiplier.

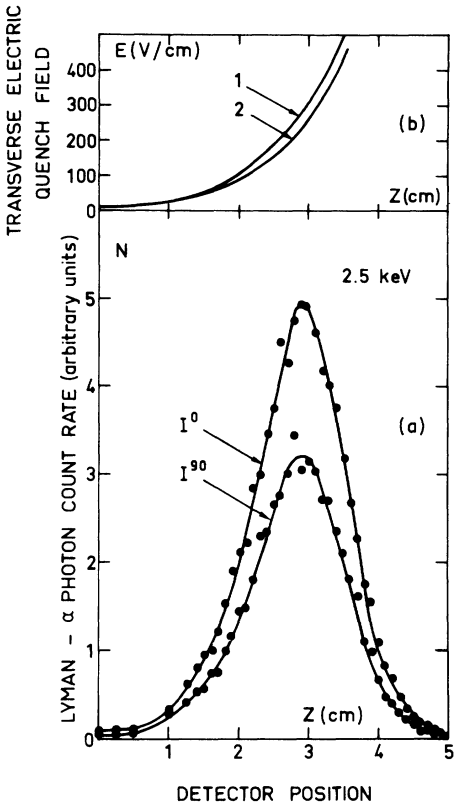

FIG. 5. (a) Lyman-α count rate (arbitrary units) for quenching of H(2S) atoms with detector parallel to (I^0) and perpendicular to (I^{90}) electric field, as a function of detector position Z along the beam axis. Incident H(2S) beam energy is 2.5 keV. (b) Calculated electric quenching field E (V/cm) as a function of detector position Z along the beam axis; the abscissa is the same for Figs. 5(a) and 5(b). Curve 1 is the result of a numerical integration of Laplace's equation. Curve 2 is the result obtained from the method described in the text, which compares the experimentally measured and the theoretical lifetimes of H(2S) atoms in an electric field.

$$\tau_m = \frac{I_m(Z)}{v} \Big/ \frac{dI_m}{dZ} = \frac{1}{vI^{\Theta}(Z)} \int_Z^{\infty} I^{\Theta}(Z')dZ'. \tag{12}$$

$I_\tau(E)$ is well known theoretically as a function of E[19]:

$$\tau_m = \tau_r \left[\left(\frac{2E}{1-(1+4E^2)^{1/2}} \right)^2 + 1 \right], \tag{13}$$

where E is in units of 475 V/cm and $\tau_r = 1.6 \times 10^{-9}$ sec is the lifetime of the radiative $2P$ states.

By combining (12) and (13) we obtain the value of the electric field as a function of $I^{\Theta}(Z)$:

$$E = (\tau_m/\tau_r - 1)^{1/2}/(\tau_m/\tau_r - 2). \tag{14}$$

To calculate E only one experimental curve $I^{\Theta}(Z)$ ($\Theta = 0°$ or 90°, for example) is needed. This method gives the electric strength with a 7% uncertainty, the primary source of error being the calculation of the integral of the signal.[57]

The two methods for determining the electric field give essentially similar results [Fig. 5(b)]. The result using Laplace's equation gives values slightly too high, which could be due to the use of plane coordinates for a problem of mixed symmetry.

Knowing the electric field at Z, the polarization is determined by measuring the photon signal with the detector successively at 0° and 90° with respect to the electric field direction. In both angular positions photons are counted during a time which is typically 1000 sec. The small background noise is measured and subtracted. Total neutral beam intensity is monitored by measuring the integral of the secondary-emission current on the neutral detector, i.e., the secondary electron total charge. The Lyman-α signal is normalized to this total charge. Thus errors due to fluctuations of the beam intensity are eliminated. According to relation (9), P is very sensitive to uncertainties in the photon signals, as the difference $I^{90} - I^{0}$ is needed to obtain P. The relative error due to counting is typically 1.5%. The error due to the monitor is 0.1% and residual misalignment of the beam can give an additional 0.5% error. Taking into account all these sources of independent error, the polarization is known with an absolute uncertainty of about 0.04, which is shown in the bars in Fig. 6. Results are shown in this figure together with predictions of adiabatic theory[33] and sudden-entry theory[34] and with previous experimental values of Sellin *et al.*[33] Our results are in reasonable agreement with the previous values and are situated in the vicinity of the adiabatic theoretical curve. The polarization of the Lyman-α radiation from the quenching of H(2S) atoms in a transverse electric field is negative, and its absolute value increases with electric field strength, reaching -0.50 ± 0.06 for a field 475 V/cm.[58] Neglecting polarization in such a field would give a photon intensity too high by a factor of 1.28 when the detection direction is parallel to the field. For a direction perpendicular to the field, the factor is 0.86. The cross section for the formation of H(2S) atoms would be in error by the same factor.

We have developed a theoretical model in order to explain the fluctuations of the experimental values about the adiabatic theoretical curve of P as a function of E (Fig. 6). In the interest of simplicity, the hyperfine structure has not been included in the model. We have numerically solved the general equation for the amplitudes of the perturbed wave function of the H($2S_{1/2}$) atom for a polynomial algebraic expression of electric field which corresponds to the actual electric field. Our theoretical curve is in agreement with the result of Sellin *et al.*[33] In addition, however, for electric fields of less than 20 V/cm, we obtain a double oscillatory structure which is related to the $2P_{3/2}$-$2S_{1/2}$ and $2P_{1/2}$-$2S_{1/2}$ splittings.[47,48] Because of the limited resolution in electric field in our experiment, this theoretically predicted double oscillatory structure is not measurable.

The experimentally measured polarization has maxima for electric field values of about 40 and 190 V/cm, and minima at about 140 and 330 V/cm.

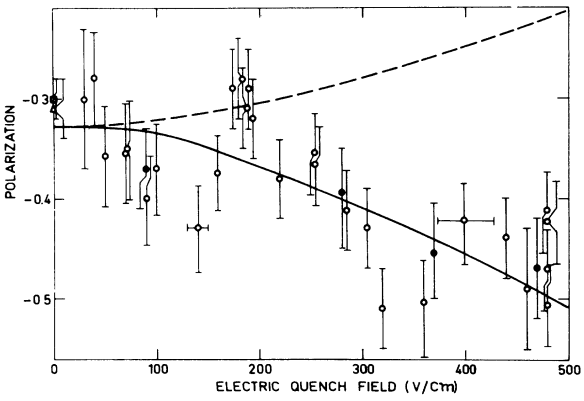

FIG. 6. Polarization of Lyman-α radiation as a function of electric quenching field. Open circles, experimental values (present experiment); closed circles experimental values (Ref. 33); squares, experimental value (Ref. 31); triangles, experimental value (Ref. 20); solid curve, adiabatic theory (Ref. 33) [our theoretical curve (Refs. 47 and 48) is identical]; broken curve, impulse theory (Ref. 34). As the detector sees a zone 5 mm long on the beam axis, the polarization measured corresponds to an average value of the electric field (horizontal error bars). The vertical error bars include all experimental uncertainties.

The electric field, which is shown as a function of detector position along the beam axis [Fig. 5(b)], corresponds to a time scale [obtained using the curve in Fig. 5(b) and the beam velocity, which is 6.9×10^{7} cm/sec]. In this manner the time intervals between the two maxima and between the two minima in Fig. 6 are found to be 1.7×10^{-8} and 1.1×10^{-8} sec.

The periods corresponding to the hyperfine structure of the $2P_{1/2}$ and $2P_{3/2}$ states are 1.69×10^{-8} sec and 4.16×10^{-8} sec, respectively. We note that the order of magnitude of the time intervals corresponding to the experimentally observed fluctuations in P is comparable to these hyperfine structure periods. It is likely that the experimentally observed fluctuations in P are related to an interference phenomenon between the radiation coming from the mixed hyperfine levels $2P_{1/2}$ and $2P_{3/2}$.

IV. CROSS SECTIONS FOR FORMATION OF H(2S) AND H(2P)

A. Experimental procedure

The error in the absolute value of our measurements of the cross section σ_{+m} is 35%. This error in the absolute value is sufficiently large to mask small variations in the relative cross-section values as a function of incident H^+ energies.

As only relative measurements are needed to study variations of σ_{+m} as a function of H^+ energy, a method was employed to eliminate the systematic uncertainties due to calibration of the Cs target thickness and of the Lyman-α detector efficiency.

In order to perform relative measurements, the H^+ energy is varied while the Cs target thickness is maintained constant. The Cs boiler is held at a constant temperature to within 0.1°C; the Cs chamber is maintained at a temperature slightly higher than the boiler and is regulated to within 1°C. The resulting variation in Cs density does not exceed 5%. The H^+ beam passes through the Cs target, which has a thickness of about 10^{13} atoms/cm^2. This is sufficiently thin so that essentially only single collisions occur. Under these conditions, it is no longer possible to measure the H^+ beam transmission β without Cs vapor. The transmission β is not 100% even in the absence of Cs because of slight misalignment and small residual fields, and it changes with H^+ energy. To eliminate the unknown transmission β, the metastable atom intensity I_m and the residual proton intensity I_+ are measured simultaneously after the collision zone. In the single collision range,

$$I_m = \beta I_+^0 \sigma_{+m} \Pi, \tag{15}$$

$$I_+ = \beta I_+^0 (1 - \sigma_{+0}\Pi), \tag{16}$$

where Π is the target thickness and σ_{+0} is the total charge-exchange cross section for formation of all neutral states of hydrogen. σ_{+0} has been measured previously.[20,21] From relations (15) and (16), β can be eliminated and σ_{+m} is obtained:

$$\sigma_{+m} = (I_m/\Pi I_+)(1 - \sigma_{+0}\Pi). \tag{17}$$

σ_{+0} is smaller than 10^{-14} cm^2; thus the term $\sigma_{+0}\Pi$ is smaller than 0.1, and uncertainty in the value of σ_{+0} does not seriously affect σ_{+m}. It is to be noted that the measured value of σ_{+m} is also insensitive to a fluctuation of the initial H^+ intensity I_+^0, since I_m and I_+ vary in the same proportion.

B. Results and discussion

Measured values of the cross section σ_{+m} for the formation of H(2S) in the energy range 0.25–3 keV are shown in Fig. 7. Between 0.25 and 1.45 keV each point shown is an average of two measurements with a D^+ beam. Between 1.3 and 3 keV each point shown is an average of four measurements with an H^+ beam. The error bars indicate only statistical uncertainty resulting from the dispersion of measured values at a given energy. A 30% additional systematic error due to calibration of the Cs detector and the Lyman-α detector

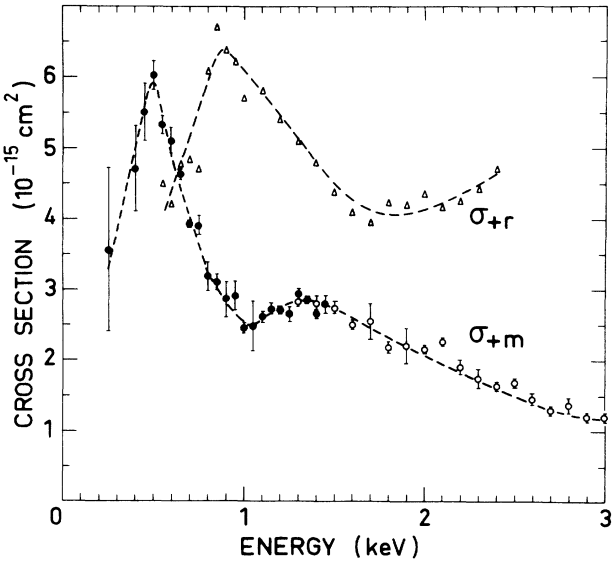

FIG. 7. Cross sections σ_{+m} and σ_{+r} for protons in cesium vapor. σ_{+m} is the cross section for electron capture in the metastable 2S state, σ_{+r} for electron capture in the radiative 2P states. σ_{+m} is directly measured in this experiment; error bars show only the relative error so as to show the existence of the maxima and minima. σ_{+r} is estimated assuming that all electron capture is in $n=2$ states. ○: incident H^+; ●: incident D^+ (shown at equivalent H^+ velocity).

must be added at each point to obtain the absolute uncertainty.

1. *Effects of scattering*

The effect of scattering is discussed in Sec. V A and in the Appendix. It appears that even with a detector acceptance angle of 0.3°, the error in the H^+ intensity I_+ is negligible for a cesium target thickness no greater than 10^{13} atoms/cm^2. The acceptance angle of the quenching system is about 1°. The scattering of metastable atoms formed by charge exchange of H^+ or D^+ with Cs atoms has yet not been experimentally studied. In a nearly resonant charge-exchange collision, the transferred momentum is small. Furthermore, it is expected that scattering of metastable atoms at angles larger than the detector acceptance angle is comparable to proton scattering, since the electron of H(2S) is far from the proton. Thus, in the absence of reliable scattering data on Cs, it is reasonable to assume that the scattering is the same for all the particles formed by charge exchange of protons in a thin Cs target. It was verified that the H^- intensity formed by double electron attachment of H^+ was negligible in a thin Cs target. With this assumption, it can be shown (Sec. V A and Appendix) that the error in I_m due to scattering would not exceed 3% for 1-keV D^+ if the metastable detector acceptance angle were 0.3°. As the real acceptance angle is three times greater, the error in I_m is certainly much smaller than 3%, and no correction has been made to the measured metastable atom intensity for the case of a thin Cs target ($\Pi = 10^{13}$ atoms/cm^2).

The cross section σ_{+0} for the formation of all the neutral states of hydrogen has been measured previously.[20,21] Direct formation of atoms in the ground state is very rare at low energy because the energy defect for the ground state is 9.7 eV, while it is only 0.5 eV for the excited states $n=2$. Thus, the difference between σ_{+0} and σ_{+m} for a given energy gives an estimation of the cross section σ_{+r} for the formation of the radiative 2P states of hydrogen. The estimation of σ_{+r} is also shown in Fig. 7.

2. *Massey criterion*

There is an evident maximum in σ_{+m} at 0.5 keV and a maximum in σ_{+r} at 0.9 keV. The well-known Massey criterion[49] provides a relationship between the velocity v_0 at the cross-section maximum and the value ΔE of the energy defect for a nonresonant charge-exchange process. For small energy defects, ΔE (eV), Drukarev[50] has shown that the bound energy I (eV) of the electron in the initial state appears in the expression of the Massey criterion. Perel *et al.*[9] have established an expression for v_0 (cm/sec),

$$v_0 = 8\times 10^7 (\Delta E/I^{1/2})^{1/2},$$

which predicts a maximum in the cross sections σ_{+m} and σ_{+r} for an energy of 0.84 keV. The predicted maximum lies between the experimentally observed maxima of σ_{+m} and σ_{+r}. By using the semiempirical wave functions of Rapp and Francis,[51] Olson *et al.*[52] have obtained a slightly different relation for v_0,

$$v_0 = 14.5\times 10^7 \Delta E/I^{1/2},$$

which predicts a maximum in the cross sections for an energy of 0.675 keV. Again, the predicted maximum is located between the observed maxima of σ_{+m} and σ_{+r}.

3. *Cascade effects*

Cascade effects from excited states with $n>2$ have to be considered. The energy defects for the states $n=3$ and $n=4$ are 2.4 and 3.0 eV, respectively. It would be expected *a priori* that the corresponding cross sections have their maxima at higher energy than for $n=2$. According to the Massey criterion, the maxima for the cross sections for electron capture into states of $n=3$ and $n=4$ are expected to occur at an energy greater than 2 keV, so the secondary maximum observed in the cross section σ_{+m} at 1.35 keV is probably not due to a cascade effect. Furthermore, the branching ratios are well known for hydrogen.[19] Only 12% of the created 3P and 4P states, and 5% of the 4S state, decay to the 2S state; the remaining atoms decay to the ground state. Thus, the influence of cascade effects is certainly small even at energies between 2 and 3 keV. However, the poorly resolved maxima observed above 2 keV in σ_{+m} could be explained by such cascade effects from the 3P, 4P, and 4S states. We assume, therefore, that the cross section σ_{+m} exhibits, between 0.5 and 1.5 keV, a structure which is due to the shape of the potential curves of the quasimolecule $(CsH)^+$. A discussion of the theoretical aspects of the collision is given in Sec. IV B 5, although the exact potential curves of $(CsH)^+$ are not yet known.

4. *Comparison with other results*

The present results for σ_{+m} compare unfavorably with those of previous experiments, which is not surprising, given the difficulty of making absolute measurements of cross sections for formation of H(2S) atoms, and noting also that previous results

differ by as much as two orders of magnitude. The results of Sellin and Granoff[3] are roughly an order of magnitude larger than the present results. This discrepancy could arise from the dubious procedure of normalizing the cross section σ_{+m} to one-quarter of the cross section σ_{+0} measured by Il'in *et al.*[22] at 10 keV. Not only is the assumption that $\sigma_{+m} = \frac{1}{4}\sigma_{+0}$ doubtful at this energy, but, furthermore, the value of σ_{+0} of Il'in *et al.* is twice as large as the value measured by Schlachter *et al.*[21] The reported values of Cesati *et al.*[2] are lower than the present results by at least a factor of 30. The reasons for this large discrepancy are not known. The results of Donnally *et al.*[1] are, on the average, roughly in agreement in magnitude with the present results, but show essentially no structure in the energy range considered. In view of the normalization procedure used and other experimental uncertainties, the apparent agreement in magnitude could be fortuitous.

The most reliable verification of the present results is a comparison made by Tuan *et al.*,[27] who used their measured values of f and reported values of σ_{+0} (Ref. 20) to calculate σ_{+m}. The results of the two experiments, obtained by two entirely independent methods, are in agreement to within the stated accuracy. This is further discussed in Sec. IV B 6, where values of f are compared.

5. *Theoretical approach*

When the two colliding partners of the initial system $H^+ + Cs$ approach each other, the energy of the quasimolecule $(CsH)^+$ changes along the $^2\Sigma^+(Cs\ 6s)$ ground state curve E_1, which is schematically represented in Fig. 8. At intermediate distances, where the total wave function of the quasimolecule changes from an atomic to a molecular basis, nonlocalized radial couplings occur between the ground state and the two lowest excited states $^2\Sigma^+(H\ 2s)$ and $^2\Sigma^+(H\ 2p_0)$ having the same molecular symmetry. The operator responsible for the transitions, in the impact parameter formulation,[16] is $\langle\psi_i|\partial/\partial R|\psi_j\rangle$, where ψ_i and ψ_j are the adiabatic molecular wave functions of the two states concerned, and where R is the interatomic distance. These excited states are correlated, along the potential curves E_2 and E_3, to the degenerate state $Cs^+ + H(n=2)$ of the separated atoms. In a first approximation, only the $2s$ and $2p_0$ orbitals of hydrogen and the $6s$ orbital of Cs are linearly combined to obtain the $^2\Sigma^+$ molecular states.

Following the analysis of Demkov,[53] the transfer of charge will occur in the vicinity of a critical distance R_c where the coupling matrix element $H_{ij}(R)$ equals one-half the difference between the intermolecular potentials $E_i(R) - E_j(R)$. By using an empirical form of $H_{ij}(R)$ established by Olson *et al.*[54] and the energy difference $E_i(\infty) - E_j(\infty) = 0.0181$ a.u. of the separated atom states, the critical distance is found to be 9.7 Bohr radii, and is the same for the two excited states E_2 and E_3. After reaching the turning point, the colliding partners separate and cross the critical region again. It is then possible to calculate approximately the transition probabilities for the two excited states by applying the well-known Demkov formulas. If no additional interaction occurred, the cross sections σ_{+m} and σ_{+r} would be determined by independently integrating these probabilities over all impact parameters.

Because the energy difference $E_2 - E_1$ is always smaller than $E_3 - E_1$, the cross section σ_{+r} would be expected to be larger than σ_{+m} for all energies. However, because the two excited states E_2 and E_3 are correlated to a degenerate state of the separated atoms, a significant coupling between them occurs at large separation due to the Coulomb effect of the Cs^+ ion,[55] so that the two-state approximation used to calculate the cross sections is insufficient. In this long-range region, the electric field $1/R^2$ can be considered as uniform in an area the size of the perturbed hydrogen atom.

The molecular wave functions of the $^2\Sigma^+$ states are well approximated by

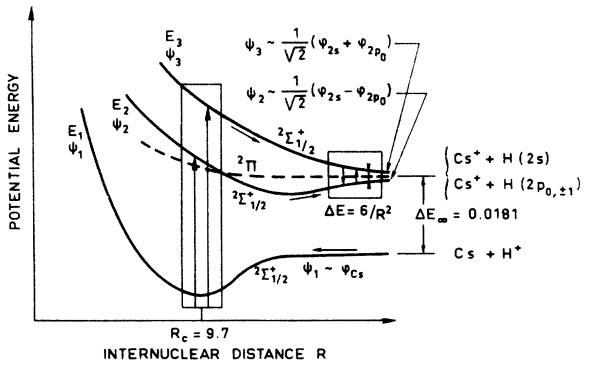

FIG. 8. Qualitative representation of the charge transfer processes involving adiabatic potential energy curves of the quasimolecule $(CsH)^+$. Preliminary results have shown that the two lowest $^2\Sigma^+_{1/2}$ states of $(CsH)^+$ are bonding while the third $^2\Sigma^+_{1/2}$ state is not bonding. The entry channel $(Cs + H^+)$ has an energy curve lower than the exit-channel curves $[Cs + H(n=2)]$, the asymptotic value of the energy difference being 0.0181 hartree. Radial coupling due to nuclear motion results from the breakdown of the Born-Oppenheimer approximation and induces transitions in the vicinity of $R_c = 9.7$ Bohr radii (long vertical arrows). At large R the two excited $^2\Sigma^+_{1/2}$ states are coupled (small vertical arrows) and their probabilities can interfere.

$$\psi_1 = \phi_{Cs}, \quad \psi_2 = \frac{1}{\sqrt{2}}(\phi_{2s} - \phi_{2p_0}),$$

$$\psi_3 = \frac{1}{\sqrt{2}}(\phi_{2s} - \phi_{2p_0}),$$

where ϕ_{Cs}, ϕ_{2s}, and ϕ_{2p_0} are the atomic wave functions of the ground state of cesium and the $2s$ and $2p_0$ states of hydrogen. It is well known from spinless Stark-effect time-dependent perturbation theory that the energy separation of the perturbed hydrogen atom will be asymptotically $E_3 - E_2 = 6/R^2$ while the coupling matrix elements are dominated by off-diagonal terms like $-3/R^2$, where R is time dependent as vt. According to this additional interaction between the two populated E_2 and E_3 states, the respective probabilities can interfere as a function of the velocity v. If there is a part of the probability phases which is not strongly dependent on the impact parameter, the interference effect can subsist after integration over all impact parameters in such a manner that the resulting σ_{+m} and σ_{+r} cross sections can exhibit oscillations in opposite phases as a function of the velocity v. Of course, the sum $\sigma_{+0} = \sigma_{+m} + \sigma_{+r}$ does not show any interference effect in that case because the total probability for transition to the two excited states remains constant.

An additional complication arises from the $^2\Pi$ molecular excited state resulting, in a first approximation, from the $2p_{\pm 1}$ orbitals of hydrogen. This excited state can be rotationally coupled to one or several molecular states of different symmetry. In fact, the separation between the region where the excited E_2 and E_3 states are populated and the region where the corresponding probabilities can interfere is not as marked as the preceding discussion assumes. A complete treatment, including the three molecular states, is necessary to interprete the observed structure of σ_{+m}.

6. *Metastable atom fraction: Comparison with other results*

The metastable atom fraction f in the outgoing neutral beam is the ratio of the number of atoms formed in the $2S$ state to the number of atoms formed in all $n=2$ states as the result of a single collision of a proton in Cs vapor. The fraction f represents the efficiency of the reaction to form metastable atoms. If cascade effects are negligible, it is equal to the ratio of the two cross sections σ_{+m} and σ_{+0}. An estimation of the fraction f is shown in Fig. 9 and is compared with direct measurements of Tuan *et al.*[27] and with lower-bound values obtained by Donnally and O'Dell.[56] The lower-bound values are determined by measurement of the D^- current after single collisions in two Cs targets, the first to form either D(1S) or D(2S) and the second to form D^-. By applying a quenching field between the two collision cells and by assuming that $\sigma_{g-} \gg \sigma_{m-}$ (σ_{g-} and σ_{m-} are the cross sections for electron capture by a D atom in the ground state and in the metastable 2S state, respectively), they found that the lower bound of f has a maximum value of 0.33 at a proton energy of 0.4 keV.

Tuan *et al.* have obtained f without calibration of the Lyman-α detector by detecting Lyman-α photons emitted from the collision region both with and without an electric quench field applied in this region. They found a maximum value $f = 0.43 \pm 0.03$ at 0.5 keV; the error bars include all sources of uncertainty except those due to polarization of the Lyman-α radiation and to cascade effects. The present work gives a value $f = 0.55 \pm 0.075$ at 0.6 keV, where the error bars include only statistical uncertainty. An additional 35% systematic error due to calibration has been discussed in Secs. IV A and IV B. The results of the present experiment, taking into account this additional 35% uncertainty, are thus seen to be in agreement with those of Tuan *et al.* The results for f of the present experiment are less accurate than those of Tuan *et al.*, as it is necessary to take the ratio of two absolute measurements, hence the large error bars. This agreement is, nonetheless, satisfying, as the two experiments used entirely different methods. We note also that the lower

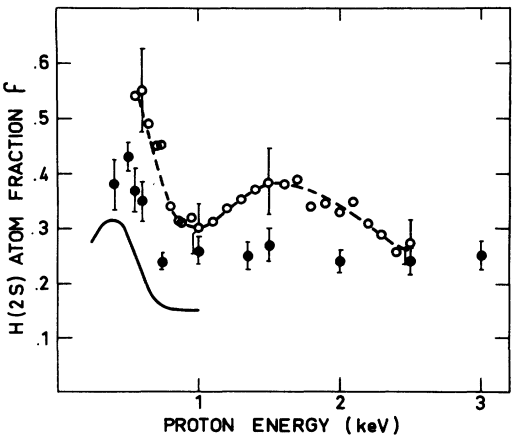

FIG. 9. Metastable atom fraction in the outgoing neutral beam as a result of a single collision of H^+ in Cs vapor. Solid curves, lower-bound values of Donnally and O'Dell (Ref. 56); closed circles, direct measurements of Tuan *et al.* (Refs. 26 and 27); open circles, present work. The three methods used to obtain f are entirely different and show a maximum value at the same energy.

bound of Donnally and O'Dell is indeed lower, and has its maximum value at the same energy as our results and those of Tuan *et al.*

It is probably justifiable to say that for H^+ energies between 0.75 and 2.5 keV, $f \sim 0.25$, which is the result to be expected if the sublevels of the $n=2$ state are statistically populated. We note that Tuan *et al.* found that $f = 0.25 \pm 0.01$ for energies between 0.75 and 3.0 keV. It is not clear from the results whether f has a maximum near 0.5 keV or whether $f \sim 0.5$ for energies ≤ 0.5 keV.

V. INFLUENCE OF MULTIPLE COLLISIONS IN THICK CESIUM TARGET

A. Experimental procedure

In order to study multiple collisions in the H^+ + Cs system, the Cs cell is slowly heated so that the Cs vapor thickness Π varies in time from 0 to 10^{15} atoms/cm^2. The intensities I'_+, I'_-, and I'_m of the three components H^+, H^-, and H(2S) are simultaneously measured as well as the secondary-emission intensity of the neutral atom detector. When corrected using the secondary-emission coefficient (Sec. III A), the neutral detector intensity gives the sum of the H(2S) atom intensity I'_m and the H(1S) atom intensity I'_g resulting from the decay of the radiative 2P states. The incident H^+ (or D^+) beam is monitored by the retractable Faraday cup located in front of the entrance of the Cs cell. Reduced component intensities I_+, I_-, I_m, and I_g are obtained by normalizing the intensity of each beam component to the initial H^+ (or D^+) intensity I^0_+ measured by the monitor. The sum of the four reduced component intensities $I_T(\Pi)$, which is the beam transmission, is then calculated and can be compared to its initial value $\beta = I_T(\Pi = 0)$. Typical variation of $I_T(\Pi)$ with Π is shown in Fig. 10 for a 1-keV incident D^+ beam (equivalent to a 0.5-keV H^+ beam). The initial transmission was 0.75. Generally $I_T(\Pi)$ exhibits a linear decrease with Π due to the scattering of the four beam components at angles larger than the detector acceptance angle. As it is not possible to investigate separately the influence of scattering for each of the four components, it is assumed that all the reduced intensities are affected in the same ratio by scattering. This is justified in the limit of a very thick Cs target, where multiple collisions take place. For a thin target, the assumption is also justified, as was discussed in Sec. IV B 1. Thus, it is for intermediate Cs target thicknesses that the assumption is less reliable. However, even in that case it can be expected that scattering of metastable atoms is comparable to proton scattering, since the electron in H(2S) is far from the proton, so that, in part, the assumption is justified. A total scattering cross section σ_T for angles larger than the detector angles can be defined from the linear variation of $I_T(\Pi)$ with Π. For a 1-keV D^+ beam, σ_T is found to be 3.10^{-16} cm^2. Finally, the four reduced intensities have been corrected in the same ratio for scattering. The fractional yields F_+, F_-, F_m, and F_g are obtained. By definition $F_+ + F_- + F_m + F_g = 1$.

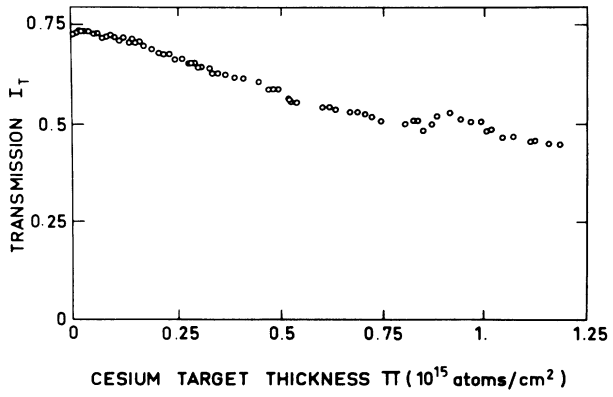

FIG. 10. Typical beam transmission vs Cs target thickness for an incident 1-keV D^+ beam (equivalent to a 0.5-keV H^+ beam). The transmission is obtained by adding the four component intensities I_+, I_-, I_m, and I_g normalized to the incident beam intensity I^0_+. The 0.75 initial transmission (without Cs vapor) results from slight misalignment and small residual fields. An average scattering cross section σ_T can be deduced from the variation of the transmission: $\sigma_T = 3 \times 10^{-16}$ cm^2.

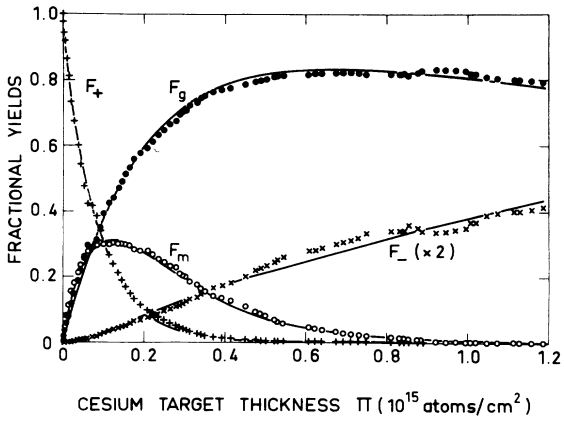

FIG. 11. Typical fractional yields as a function of Cs target thickness π for an incident 1-keV D^+ beam. The yields F_+, F_m, F_g, and F_- (shown multiplied by 2) are the fractions of the beam in the positive, metastable 2S, ground, and negative charge states, respectively. The H(2S) fractional yield exhibits a maximum and goes to a near-zero equilibrium value for infinite thickness, indicating the predominance of collisional destruction of H(2S) atoms.

B. Results and discussion

Typical fractional yields obtained as a function of Cs target thickness Π are shown in Fig. 11 for incident 1 keV D^+. In the given energy range (0.5–2.5 keV), the experimental data representing the fractional yield for each component have the same form as in Fig. 11. When Π increases one notes an exponential decrease of the H^+ fractional yield F_+. Simultaneously the H(2S) fractional yield F_m increases (Fig. 12). When Π is much larger than 10^{13} atoms/cm² multiple collisions are not negligible and the metastable atoms can be collisionally deexcited. F_m increases nonlinearly with Π up to a maximum value. This maximum value increases with decreasing energy. The maximum of F_m occurs for a Cs target thickness of about 1.2×10^{14} atoms/cm². The values of the maximum of F_m are shown in Table I with a 35% uncertainty. It is to be noted that a maximum of 31% of the incident D^+ beam can be transformed into metastable atoms at 1 keV. For values of Π above that at which the maximum occurs F_m decreases and apparently goes to a near-zero equilibrium value, indicating the predominance of collisional destruction of the metastable atoms. The ground-state fractional yield F_g and the negative fractional yield F_- increase monotonically with Π. In the vicinity of $\Pi = 6\times10^{14}$ atoms/cm², F_g reaches a limiting value which is greater than 0.80 in the studied energy range. The negative fractional yield F_- exhibits behavior typical of a two-step process, as shown in Fig. 11. In the Cs target-thickness range studied, F_- does not reach an equilibrium value, contrary to what would be expected. The reason for this might be that the effect of scattering has not been correctly taken into account, or that there is secondary-electron emission on the guard ring of the Faraday cup. In any case, F_- is small, and does not have an important influence on the accuracy of the other three fractional yields.

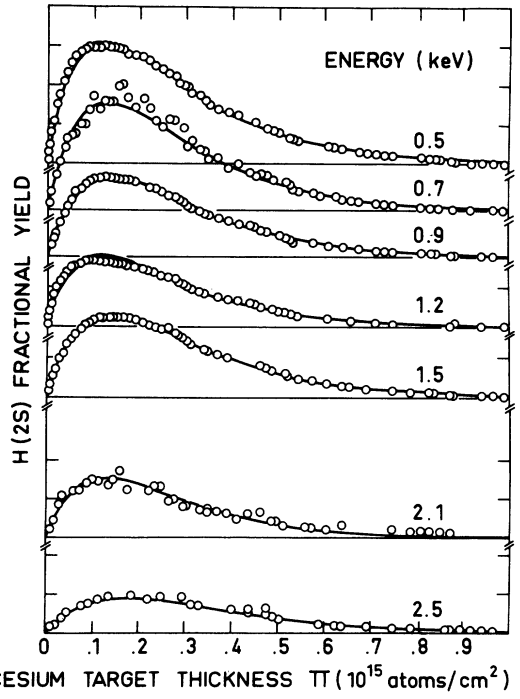

FIG. 12. H(2*S*) fractional yield as a function of Cs target thickness π for incident H^+ energies between 0.5 and 2.5 keV. The H(2*S*) fraction shown in this figure is the fraction of outgoing beam in the 2*S* state relative to the *total* outgoing beam, and is not to be confused with the metastable fraction f relative to the outgoing ***neutral*** beam shown in Fig. 9. The position of the curves along the ordinate axis is proportional to the energy, thus permitting interpolation for a energy not shown. One division along the ordinate corresponds to a 10% fractional yield. The curve shown as 0.5 keV H^+ energy was actually D^+ at 1 keV.

We have calculated the destruction cross section for metastable atoms by use of the charge-exchange differential equation. The four component charge-exchange differential equations are integrated, and a nonlinear least-square analysis is used to fit the calculated fractional yields to the experimental data, which determines values for the cross sections. The calculated fractional yields are shown as solid curves in Fig. 11 for incident 1-keV D^+. The apparent agreement between the calculated fractional yields and the experimental data has to be considered cautiously, since it proves neither the correctness of the experimental data nor the correctness of the obtained cross-section values. With this method, the accuracy of the calculated cross sections is difficult to estimate. Scattering is probably the main source of error in the experimental data. Thus, it seems reasonable to assume that an upper bound on the error in calculated cross sections is the total scattering cross section σ_T measured by adding the four fractional-yield components. The calculated cross sections

TABLE I. Maximum fractional yield of H atoms in the metastable 2*S* state after charge exchange of H^+ in Cs vapor, relative to total beam after passage through the target.

Proton energy (keV)	Maximum metastable fractional yield
0.5(D^+: 1.0)	0.31
0.7	0.27
0.9	0.20
1.2	0.18
1.5	0.21
2.1	0.15
2.5	0.09

having values less than σ_T are assumed to be insignificant. As was pointed out in Ref. 20, calculation shows that the primary destruction cross section for metastable atoms in Cs is the deexcitation cross section σ_{mg}, which is about 5×10^{-15} cm^2 in our energy range. The electron attachment cross section σ_{m-} is an order of magnitude lower, and the detachment cross section σ_{m+} is not measurable by this technique.

ACKNOWLEDGMENTS

We would like to thank Dr. C. Manus and Dr. G. Watel for their kind assistance. One of us (A.S.) gratefully acknowledges a Joliot-Curie Fellowship from the Institut National des Sciences et Techniques Nucléaires at Saclay.

APPENDIX: ERRORS IN THE MEASURED INTENSITIES IN A THIN CESIUM TARGET

For a thin cesium target and for detector acceptance angle θ (half angle) the measured reduced intensities are

$$I_+ = 1 - \Pi(\sigma_{+m}+\sigma_{+g}) - \Pi\int_\theta^\pi \frac{d\sigma_+}{d\Omega}\,d\Omega,$$

$$I_m = \Pi\int_0^\theta \frac{d\sigma_{+m}}{d\Omega}\,d\Omega,$$

$$I_g = \Pi\int_0^\theta \frac{d\sigma_{+g}}{d\Omega}\,d\Omega,$$

where $d\sigma_{+i}/d\Omega$ are the differential inelastic cross sections for formation of beam components i, and $d\sigma_+/d\Omega$ is the differential elastic cross section for protons in cesium. The direct formation of H^- (double electron attachment) may be neglected, as shown in Fig. 11. The total measured reduced intensity is

$$I_T = I_+ + I_m + I_g = 1 - \Pi\int_\theta^\pi \left(\frac{d\sigma_{+m}}{d\Omega}+\frac{d\sigma_{+g}}{d\Omega}+\frac{d\sigma_+}{d\Omega}\right)d\Omega$$
$$= 1 - \Pi\sigma_T,$$

where $\Pi\sigma_T$ is the loss of total intensity and can be easily measured (Fig. 10). The absolute errors due to scattering of each intensity are, respectively,

$$\Delta I_+ = \Pi\int_\theta^\pi \frac{d\sigma_+}{d\Omega}\,d\Omega,$$

$$\Delta I_m = \Pi\int_\theta^\pi \frac{d\sigma_{+m}}{d\Omega}\,d\Omega,$$

$$\Delta I_g = \Pi\int_\theta^\pi \frac{d\sigma_{+g}}{d\Omega}\,d\Omega,$$

so that $\Delta I_+ + \Delta I_m + \Delta I_g = \Pi\sigma_T$.

According to the discussion in Secs. VI B and V A, if one assumes that scattering is similar for the three beam components at angles greater than the detector acceptance angle, the following relation applies:

$$\int_\theta^\pi \frac{d\sigma_+}{d\Omega}\,d\Omega/\sigma_+ = \int_\theta^\pi \frac{d\sigma_{+m}}{d\Omega}\,d\Omega/\sigma_{+m}$$
$$= \int_\theta^\pi \frac{d\sigma_{+g}}{d\Omega}\,d\Omega/\sigma_{+g} = \frac{\sigma_T}{\sigma_+ + \sigma_{+m} + \sigma_{+g}}.$$

In the sum $\sigma_+ + \sigma_{+m} + \sigma_{+g}$ the total elastic cross section σ_+ is comparable to σ_T and is negligible compared to $\sigma_{+m} + \sigma_{+g} = \sigma_{+0}$ so that the error of the intensities can be estimated:

$$\Delta I_+ \sim \Pi\sigma_+\sigma_T/\sigma_{+0}, \quad \Delta I_m \sim \Pi\sigma_{+m}\sigma_T/\sigma_{+0},$$

$$\Delta I_g \sim \Pi\sigma_{+g}\sigma_T/\sigma_{+0}.$$

The relative errors are

$$\Delta I_+/I_+ \sim \Pi\sigma_+\sigma_T/\sigma_{+0} \sim \Pi\sigma_T^2/\sigma_{+0},$$

$$\frac{\Delta I_m}{I_m} \sim \frac{\Pi\sigma_{+m}\sigma_T}{\sigma_{+0}\Pi(\sigma_{+m} - \sigma_{+m}\sigma_T/\sigma_{+0})} = \frac{\sigma_T}{\sigma_{+0}-\sigma_T},$$

$$\Delta I_g/I_g \sim \sigma_T/(\sigma_{+0}-\sigma_T).$$

For $\Pi = 10^{13}$ atoms/cm^2 and for 1-keV deuterons, the measured cross-section values are $\sigma_T = 3\times10^{-16}$ cm^2, $\sigma_{+0} = 1\times10^{-14}$ cm^2; thus

$$\Delta I_+/I_+ \sim 0.1\%, \quad \Delta I_m/I_m = \Delta I_g/I_g \sim 3\%.$$

An upper bound for $\Delta I_m/I_m$ may be obtained by assuming that the total scattering is due only to the metastable atoms. In this condition, the error would be

$$\Delta I_m/I_m \sim \sigma_T/(\sigma_{+m}-\sigma_T) \sim 5.5\%.$$

[1] B. L. Donnally, T. Clapp, W. Sawyer, and M. Schultz, Phys. Rev. Lett. 12, 502 (1964).
[2] A. Cesati, F. Cristofori, L. Millazo Colli, and P. G. Sona, Nucl. Energy 13, 649 (1966).
[3] I. A. Sellin and L. Granoff, Phys. Lett. A 25, 484 (1967).
[4] W. Haeberli, Annu. Rev. Nucl. Sci. 17, 406 (1967).
[5] B. L. Donnally and W. Sawyer, Phys. Rev. Lett. 15, 439 (1965).
[6] M. Bruckmann, D. Finken, and L. Friedrich, Phys. Lett. B 29, 223 (1969).
[7] L. D. Knutson, Phys. Rev. A 2, 1878 (1970).
[8] J. Perel, Phys. Rev. A 1, 369 (1970).
[9] J. Perel and H. L. Daley, Phys. Rev. A 4, 162 (1971).
[10] J. R. Peterson and D. C. Lorents, Phys. Rev. 182, 152 (1969).
[11] J. Perel and H. L. Daley, Phys. Rev. A 1, 1626 (1970).

[12]D. Storm and D. Rapp, J. Chem. Phys. 53, 1333 (1970).
[13]C. Bottcher and M. Oppenheimer, J. Phys. B 5, 492 (1972).
[14]C. F. Melius and W. A. Goddard, Chem. Phys. Lett. 15, 524 (1972).
[15]C. F. Melius and W. A. Goddard, Phys. Rev. Lett. 29, 975 (1972).
[16]D. R. Bates and R. McCarroll, Proc. R. Soc. A 245, 175 (1958).
[17]A. Dalgarno, C. Bottcher, and G. A. Victor, Chem. Phys. Lett. 7, 265 (1970).
[18]W. L. McMillan, Phys. Rev. A 4, 69 (1971).
[19]H. E. Bethe and E. E. Salpeter, *Quantum Mechanics of One and Two Electron Atoms* (Academic, New York, 1957).
[20]G. Spiess, A. Valance, and P. Pradel, Phys. Rev. A 6, 746 (1972).
[21]A. S. Schlachter, P. J. Bjorkholm, D. H. Loyd, L. W. Anderson, and W. Haeberli, Phys. Rev. 177, 184 (1969).
[22]R. N. Il'in, V. A. Oparin, E. S. Solov'ev, and N. V. Fedorenko, Zh. Tekh. Fiz. 36, 1241 (1966) [Sov. Phys. - Tech. Phys. 11, 921 (1967)].
[23]G. Spiess, A. Valance, and P. Pradel, Phys. Lett. A 31, 434 (1970).
[24]W. Grüebler, P. A. Schmelzbach, V. König, and P. Marmier, Helv. Phys. Acta 43, 254 (1970).
[25]W. Grüebler, P. A. Schmelzbach, V. König, and P. Marmier, Phys. Lett. A 29, 440 (1969).
[26]Vu Ngoc Tuan, A. S. Schlachter, and G. Gautherin, Nucl. Instrum. Methods 114, 499 (1974).
[27]Vu Ngoc Tuan, G. Gautherin, and A. S. Schlachter, Phys. Rev. A 9, 1242 (1974).
[28]R. L. Fitzwilson and E. W. Thomas, Phys. Rev. A 3, 1305 (1971).
[29]R. L. Fitzwilson and E. W. Thomas, Phys. Rev. A 6, 1054 (1972).
[30]W. L. Fite, W. E. Kaupilla, and W. R. Ott, Phys. Rev. Lett. 20, 409 (1968).
[31]W. R. Ott, W. E. Kaupilla, and W. L. Fite, Phys. Rev. A 1, 1089 (1970).
[32]J. Casalese and E. Gerjuoy, Phys. Rev. 180, 327 (1969).
[33]I. A. Sellin, J. A. Biggerstaff, and P. M. Griffen, Phys. Rev. A 2, 423 (1970).
[34]D. H. Crandall and D. H. Jaecks, Phys. Rev. A 4, 2271 (1971).
[35]J. W. Wooten and J. M. Macek, Phys. Rev. A 5, 137 (1972).
[36]E. S. Chambers, Phys. Rev. 133, A1202 (1964).
[37]P. M. Stier, C. F. Barnett, and G. E. Evans, Phys. Rev. 96, 973 (1954).
[38]R. Dagnac, D. Blanc, and D. Molina, J. Phys. B 3, 1239 (1970).
[39]S. N. Ghosh and S. P. Khare, Phys. Rev. 125, 1254 (1962).
[40]C. F. Barnett and J. A. Ray, Rev. Sci. Instrum. 43, 218 (1972).
[41]P. Pradel, F. Roussel, and G. Spiess, Rev. Sci. Instrum. 45, 49 (1974).
[42]D. Jaecks, B. Van Zyl, and R. Geballe, Phys. Rev. 137, A340 (1965).
[43]E. P. Andreev, V. A. Ankudinov, and S. V. Bobashev, Zh. Eksp. Teor. Fiz. 50, 565 (1966) [Sov. Phys.—JETP 23, 375 (1966)].
[44]J. E. Bayfield, Phys. Rev. 182, 115 (1969).
[45]M. Kaminsky, *Atomic and Ionic Impact Phenomena on Metal Surfaces* (Springer, Berlin, 1965), p. 324.
[46]D. H. Crandall, R. H. McKnight, and D. H. Jaecks, Phys. Rev. A 7, 1261 (1973); for very small angles, their results have been extrapolated by using a scattering law resulting from a long-range interaction in $1/R^4$, where R is the interatomic distance between H^+ and Ar.
[47]P. Pradel, F. Roussel, A. S. Schlachter, G. Spiess, and A. Valance, Phys. Lett. A 44, 55 (1973); this aperture was incorrectly given here as 20 mm.
[48]A. Valance, P. Pradel, F. Roussel, A. S. Schlachter, and G. Spiess, in *Proceedings of the Eighth International Conference on the Physics of Electronic and Atomic Collisions, Belgrade, 1973,* edited by B. C. Cobic and M. V. Kurepa (Institute of Physics, Beograd, 1973), p. 653.
[49]H. S. W. Massey, Rep. Prog. Phys. 12, 248 (1949).
[50]G. F. Drukarev, in *Proceedings of the Fifth International Conference on the Physics of Electronic and Atomic Collisions, Leningrad, 1967,* edited by I. P. Flaks and E. S. Solovyov (Leningrad, Nauka, 1967).
[51]D. Rapp and W. E. Francis, J. Chem. Phys. 37, 2631 (1962).
[52]R. E. Olson, Phys. Rev. A 6, 1822 (1972).
[53]Yu. N. Demkov, Zh. Eksp. Teor. Fiz. 45, 195 (1963) [Sov. Phys.—JETP 18, 138 (1964)].
[54]R. E. Olson, F. T. Smith, and E. Bauer, Appl. Opt. 10, 1848 (1971).
[55]L. Wilets and D. F. Gallaher, Phys. Rev. 147, 13 (1966).
[56]B. L. Donnally and J. E. O'Dell, in *Proceedings of the Seventh International Conference on the Physics of Electronic and Atomic Collisions, Amsterdam, 1971,* edited by L. M. Branscomb, H. Ehrhardt, R. Geballe, F. J. de Heer, N. V. Fedorenko, J. Kistemaker, M. Barat, E. E. Nikitin, and A. C. H. Smith (North-Holland, Amsterdam, 1971), p. 821. The result cited for f should be a D^+ energy of 800 eV, not H^+ at 800 eV [B. L. Donnally (private communication)].
[57]We have verified that the electric field calculated by using either $I^0(Z)$ or $I^{90}(Z)$ is the same.
[58]This is contrary to the preliminary result given in Ref. 20 which was incorrect because the Lyman-α detector was not diaphragmed sufficiently to avoid a shadow effect from the quenching plates in the strong electric field region.